ELSEVIER

Polymer 42 (2001) 1407–1416

polymer

www.elsevier.nl/locate/polymer

Crystallinity and morphology of PVdF–HFP-based gel electrolytes

S. Abbrent[a], J. Plestil[b], D. Hlavata[b], J. Lindgren[a], J. Tegenfeldt[a,*], Å. Wendsjö[c]

[a]*The Ångström-Laboratory, Inorganic Chemistry, Uppsala University, Box 538, SE-751 21 Uppsala, Sweden*
[b]*Institute of Macromolecular Chemistry, Academy of Science of the Czech Republic, Heyrovsky Sq. 2, 162 06 Prague, Czech Republic*
[c]*Danionics A/S, Hestehaven 21j, DK-5260 Odense S, Denmark*

Received 7 April 2000; received in revised form 25 June 2000; accepted 10 July 2000

Abstract

The structural behaviour of a random copolymer consisting of polyvinylidene fluoride (PVdF) and hexafluoropropylene (HFP), when mixed with organic solvents and a lithium salt, has been investigated. In its neat form, the copolymer exhibits a semicrystalline matrix, where the PVdF constituent crystallises partially. The crystalline phase appears mostly as the non-polar (*trans–gauche–trans–gauche′*) phase II. The relative crystallinity of the PVdF domains remains constant on addition of a plasticiser, propylene carbonate (PC) or triethylene glycol dimethyl ether (TG), but is greatly decreased on addition of the salts lithium bis(trifluoromethane sulfone) imide, Li(TFSI) or lithium tetrafluoroborate, $LiBF_4$. This is shown by the results from both wide-angle (WAXS) and small-angle (SAXS) X-ray scattering and FTIR-spectroscopy. Surprisingly, the addition of such a polar medium as the salt, and to a lesser extent the plasticisers, also causes a change in the structure of the crystalline phase to a more polar phase III (intermediate polar conformation). The thermal stability of the gels and the large influence the salt addition has on the material is also shown by the results from differential scanning calorimetry (DSC) measurements.

Keywords: Crystallinity; Morphology; Polyvinylidene fluoride–hexafluoropropylene-based gel electrolytes

1. Introduction

Polyvinylidene fluoride (PVdF), the main constituent of the copolymer used in this work, has been known since the 1960s for its excellent mechanical properties and it has since found its way to many research areas and industrial uses [1]. Its piezoelectricity has been widely investigated [2–5], and several research groups have been committed to the resolving of its complex morphology, finding several different crystalline phases [6–11]. Phase II (or α) has a non-polar *trans–gauche–trans–gauche′* (TGTG′) conformation, and it is the most common phase, appearing under normal circumstances. The polar crystalline phase I (or β) has a zig-zag (all *trans*) conformation and it results when the polymer is strained, stretched or quenched. Phase III (or γ) has an intermediate polar TTTGTTTG′ [12] conformation, occurring when the polymer is moderately stressed. The last phase IV (or δ) appears only under special crystallisation temperatures and pressures.

The PVdF itself is highly crystalline. When copolymerised with hexafluoropropylene (HFP), the degree of crystallinity is greatly reduced [13]. This changes the mechanical properties of the resulting copolymer, i.e. its flexibility is greatly enhanced as compared to neat PVdF [14,15]. The copolymer has been shown to be a promising matrix for an electrolyte material in modern lithium ion batteries. The crystallinity remaining in the system retains sufficient mechanical stability to allow it to act, for example, as a separator between the electrodes of a battery, while the amorphous phase can contain the conductive medium, in this case a liquid electrolyte [13].

Preparation of a so-called gel electrolyte based on this type of polymer involves the admixture of a plasticizing solvent and a salt into the polymer matrix. Depending on the type and amount of salt and solvent(s) present in the polymer matrix, the morphology of the polymer will vary and greatly influence the properties of the gel electrolyte [16–20]. To understand the interactions between the salt, the solvent and the polymer is therefore crucial, because the knowledge of the morphology and its changes is important for obtaining an electrolyte with good mechanical properties. For example, the electrolyte must not melt within the operational temperature regime of the battery and thereby short-circuit the system, or repel the conductive medium at lower temperatures and in that way act as an insulator.

The local interactions among the salt, solvent and polymer have recently been investigated by us using FTIR

* Corresponding author. Tel./fax: +46-18-47-13774.
E-mail address: jorgen.tegenfeldt@kemi.uu.se (J. Tegenfeldt).

0032-3861/01/$ - see front matter
PII: S0032-3861(00)00517-6

spectroscopy [21]. In those studies, the relative amount of the lithium ions coordinating to solvent molecules was found to be the same with or without polymer added to the system. It was therefore concluded, that there were no local interactions between the polymer and the solvent. Some changes in the spectra, which were not analysed at the time, have prompted us to investigate these systems further.

Because of the complexity of the system one is required to use several experimental techniques together in order to fully grasp its complicated behaviour. While small-angle X-ray diffraction (SAXS) shows the long-range order and morphology, wide-angle X-ray diffraction (WAXS) focuses on the crystalline part, its structure and relative amount in a sample. Infrared spectroscopy (FTIR) can then clearly distinguish between different crystalline phases occurring. Some of the final macromolecular properties of a gel can be established by a thermal analysis, in the present case by differential scanning calorimetry (DSC). Changing the composition of the gels gives furthermore an understanding of the relative influence of the components on the resulting material.

2. Experimental

2.1. Material preparation

The polymer powder used as a starting material was purchased at Elf Atochem under the trade name Kynar flex 2801 (the abbreviation for the copolymer used in the figures is therefore KF). This particular polymer contains 12 wt% of HFP stochastically incorporated into the vinylidene fluoride backbone (a random copolymer). On preparation of the samples, the polymer powder was mixed with various amounts of a plasticiser, propylene carbonate (PC) (Merck, >99%) or triethylene glycol (TG) (Aldrich, >99%), or a 1 M salt solutions in these plasticisers, and dissolved in an excess of acetone (Baker analysed, >99.7%). The salt used was lithium bis(trifluoromethane sulfonyl)imide, LiTFSI (3M Ltd) or lithium tetrafluoroborate, $LiBF_4$, (Tomiyama, Battery grade). The final samples were made to contain 0–100 wt% of the plasticiser or the salt solution.

Films were prepared in a glove-box at room temperature by the solvent casting method, and left to dry there over night to evaporate all the solvent. The completeness of solvent removal was checked by differential scanning calorimetry and by FTIR spectroscopy (see below). All samples and films were kept in a nitrogen-filled glove-box in order to avoid water contamination. Prior to the gel preparation, the plasticisers were also dried by the appropriate molecular sieve (4 Å), while the salts were dried in a vacuum oven at 100°C for 48 h, and possible contamination by water was checked by infrared spectroscopy (peak at 3500 cm^{-1}).

2.2. Small-angle X-ray scattering (SAXS)

A Kratky camera equipped with a position-sensitive detector has been used in this study on the same samples used for the WAXS measurements as described below. Scattering intensities are presented as a function of the magnitude of the scattering vector $q = (4\pi/\lambda)\sin\theta$, where λ is the wavelength of the radiation and 2θ is the scattering angle. Due to slit collimation, the experimental (smeared) scattering curves had to be corrected for collimation effects. The desmearing program ITR developed by Glatter and Gruber [22] was used. The scattering curves were put on an absolute scale using a Lupolen standard [23]. However, due to the non-uniformity of the sample thickness, the absolute scale is not reliable enough for applying the procedures relying on absolute intensities. In determining periodicity of lamellar structures Lorentz-corrected SAXS curves [24] ($q^2I(q)$ versus q) were used.

2.3. Wide-angle X-ray scattering (WAXS)

The diffractograms of the samples were taken on an automatic powder diffractometer HZG/4A. The CuK_α radiation was monochromatised by a Ni filter and an amplitude analyser, and recorded by means of a scintillation counter. The diffractograms were recorded in the range of the diffraction angle $2\theta = 4$–$60°$. In order to protect the films from moisture during the four hour data accumulation, the samples were enclosed in aluminium foil and then sealed in a plastic bag. A window was cut out in the plastic bag so that the scattering from the plastic material would not disturb the resulting diffractograms. Two sharp reflections at $2\theta = 37.9$ and 38.3° from Al made it impossible to use the whole range of the diffractograms for the calculation of the degree of crystallinity in the samples. Instead, the relative changes of the crystallinity derived from the data in the range of $2\theta = 5$–$30°$ are reported.

2.4. Differential scanning calorimetry (DSC)

The thermal stability and morphology of the films have been investigated with a Mettler model DSC20 oven connected to a Mettler TA4000 controller. All samples, sealed in a glove-box into aluminium cans, were cooled down to −150°C with liquid nitrogen, and then heated up to 300°C, both at the rate of 10°C min^{-1}. The presence of acetone in the samples could be clearly dismissed from the absence of the broad peak expected around the boiling point at 60°C.

2.5. Fourier transform infrared spectroscopy (FTIR)

The infrared spectra were recorded under nitrogen atmosphere on a Digilab-Biorad FTS-45 spectrometer, covering a range of 400–4400 cm^{-1} with a resolution of 2 cm^{-1}. The films were cast directly on a KBr window allowing sufficient time for the acetone to evaporate fully before each spectrum was acquired. Also, there were no signs of a carbonyl band from residual acetone around 1700 cm^{-1}.

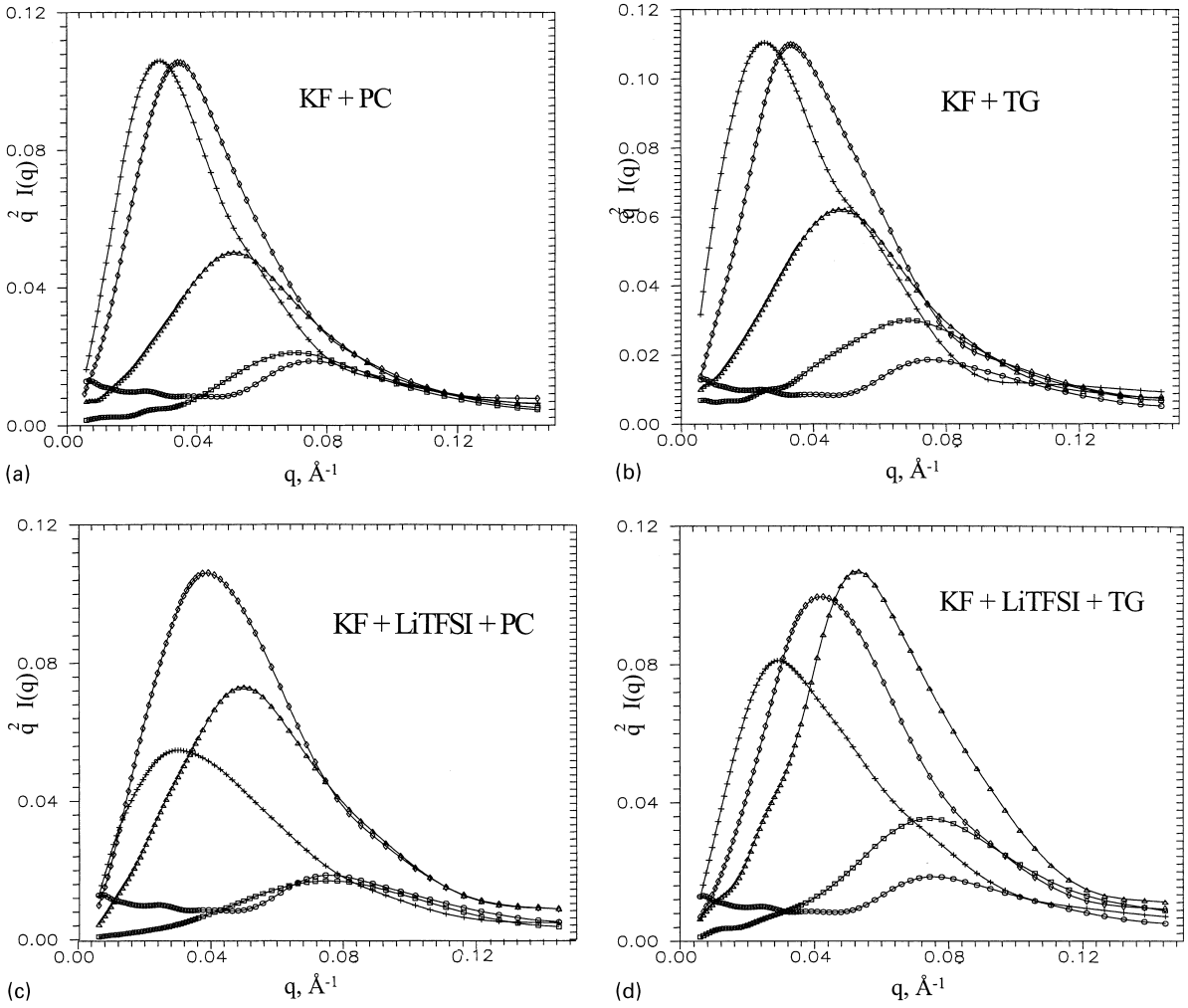

Fig. 1. The Lorentz-corrected SAXS curves, where (○) symbolises the neat polymer, (□) 10%; (▽) 30%; (◇) 50%; and (+) 70% of plasticiser added. In (a) the plasticiser is PC; in (b) TG; in (c) 1 M LiTFSI in PC; and in (d) 1 M LiTFSI in TG.

3. Results and discussion

3.1. SAXS

X-ray scattering at low angles enables an insight into the morphology of the system. Heterogeneities caused by differences in density distributed over the polymer film sample, such as periodically repeating crystalline and amorphous regions, can be revealed. Also, the mean distance between crystalline regions can be resolved. In our case, this can be used to study the influence of the gradual addition of plasticisers and salt on the morphology of the copolymer.

The SAXS curves of most of the samples (especially those with low content of plasticiser) exhibit one broad maximum. This feature is typical for semicrystalline polymers [24] and reflects a certain periodicity of the system. The SAXS technique itself cannot provide any decisive information on the structure in this case. We assume a lamellar structure model with parallel crystalline lamellae separated by amorphous layers. The structure will be characterised by the long period, L, calculated as

$$L = 2\pi/q^*$$

where q^* is the position of the maximum of the Lorentz-corrected SAXS intensity. The data from the SAXS measurements are displayed in Fig. 1 as $q^2I(q)$ versus q. For the neat copolymer, the long period was estimated to be $L = 84$ Å.

The addition of the plasticisers to the polymer matrix leads to a shift in the position of the maximum to lower scattering vectors (L increases) (Fig. 1a and b). This increase of the long period can be correlated with increasing amounts of the plasticisers added. The experimental values of L are similar to theoretical ones, L_{th} (Fig. 2) based on a simple one-dimensional dilution model involving expansion normal to the lamellar planes. Here $L_{th} = L_p/(1 - v_{pl})$ (L_p is the long period for pure copolymer = 84 Å and v_{pl} is the volume fraction of plasticiser added, calculated using the densities 1.6 for neat copolymer, 1.29 for PC and 0.98 g cm^{-3} for TG). The long periods do not seem to be

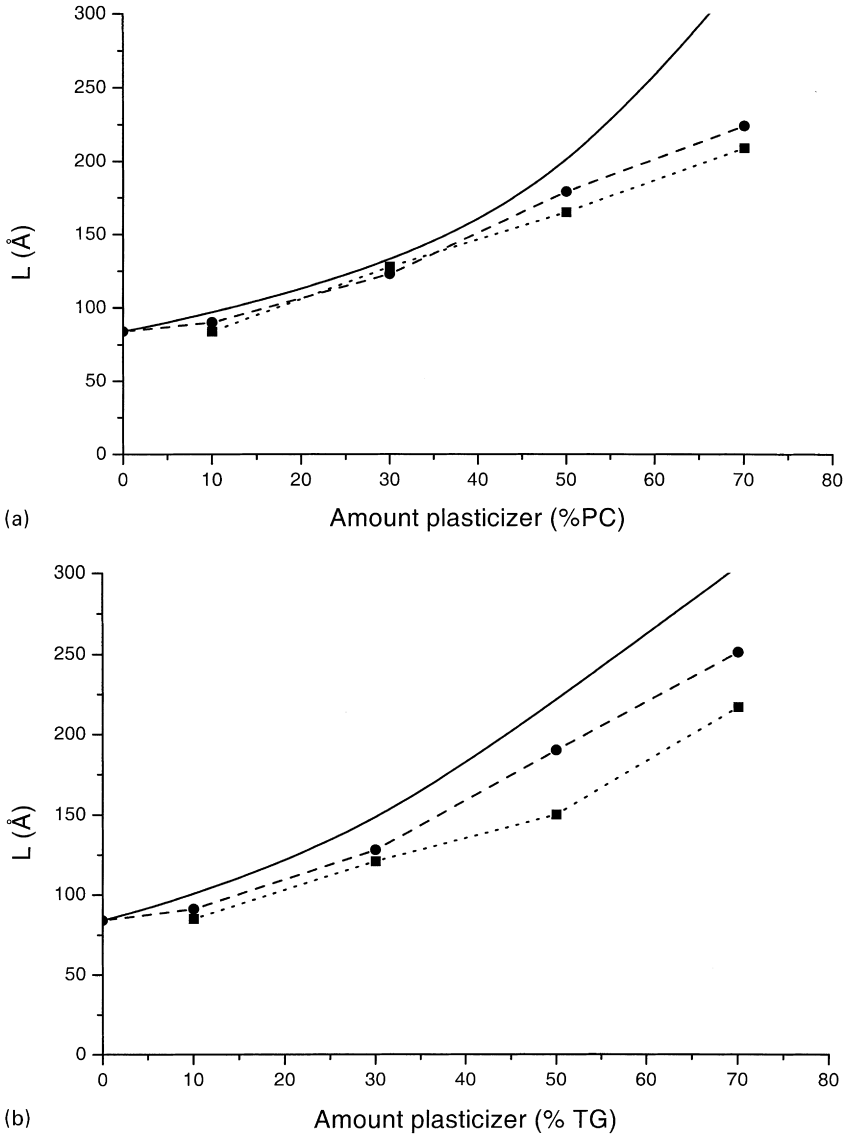

Fig. 2. A graph showing the growth of the lamellar distance L on plasticiser addition. In the systems in (a) the plasticiser is PC and in (b) TG. The smooth line represents the theoretical values L_{th}, the dashed line connects the data points for the system with plasticiser addition and the dotted line the values for the system with salt and plasticiser added.

dramatically influenced by the nature of the plasticiser or by the addition of salt, except at high concentrations (50–70%). However, the addition of salt broadens the maxima of the SAXS data (Fig. 1c and d). This points to imperfections in the periodicity and parallelism of the crystalline lamellae in the samples.

3.2. WAXS

Wide-angle diffraction measurements reveal short-range periodicity in the crystalline parts of the samples. Here, therefore, information about the structure of the crystalline phase can be derived and the influence of plasticiser and salt on the crystalline phase of PVdF and its structure can be investigated. It is also possible to calculate the ratio of the crystalline to amorphous regions by profile analysis. A more detailed information on the morphology than by using the SAXS technique can therefore be obtained.

The PVdF–HFP copolymer samples of all compositions used have a semicrystalline morphology. The separation of the crystalline reflections from the broad peak, a halo, from the amorphous phase, has been performed by profile analysis using the program by Petkov and Bakalatchev [25]. The results from this analysis were used for the calculation of the total crystallinity of the samples, w_{cr}, i.e. the mass fraction of the crystalline phase relative to the total mass of the sample. It was determined using the formula [26]

$$w_{cr} = \int_0^\infty I_{cr}(q)q^2\,dq / \int_0^\infty I(q)q^2\,dq$$

where I_{cr} is the intensity scattered by the crystalline domains, I the overall scattered intensity, $q = (4\pi/\lambda)\sin\theta$

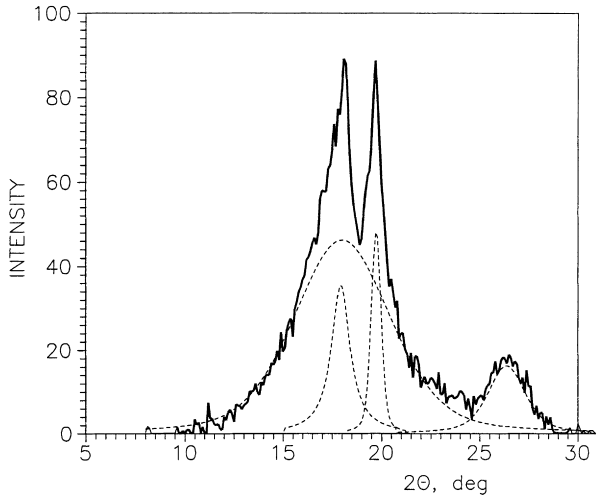

Fig. 3. A WAXS diffractogram of the neat copolymer showing the results of the profile analysis (solid line), where the resolved individual reflections are shown (dashed line).

is the magnitude of the scattering vector, λ the wavelength of the radiation, and 2θ the scattering angle. This relation is strictly speaking valid only if the scattering material is the same in the amorphous and crystalline regions, thus it is valid only approximately in the present case. From w_{cr} simple stoichiometric considerations give the relative crystallinity, $(w_{cr})_{KF}$, defined as the mass fraction of crystalline PVdF relative to the total copolymer mass.

Profile analysis of the wide-angle diffractogram for the neat copolymer (Fig. 3) reveals three strong peaks of the crystalline phase at the diffraction angles $2\theta = 18.4$, 20.0, and 26.7°, and a broad amorphous halo with centre at $2\theta = 18.0°$. The crystalline peaks can be associated with the reflections (100) + (020), (110), and (021), respectively, typical for the orthorhombic cell of neat PVdF in its crystalline form II, where $a = 4.96$, $b = 9.64$, and c (the chain axis) = 4.62 Å. [8,27]. This confirms that the PVdF units in the copolymer are capable of a partial crystallisation.

Table 1
Structure parameters of polymer blends (w_{cr}, overall degree of crystallinity; $(w_{cr})_{KF}$, crystallinity of the PVdF matrix; $2\theta_{am}$, position of the amorphous halo; $(2\theta)_1$, $(2\theta)_2$ and $(2\theta)_3$, positions of the crystalline reflections; w_1 and w_2, corresponding half-widths of the reflections (relative scale))

	w_{cr}	$(w_{cr})_{KF}$	$2\theta_{am}$	$(2\theta)_1$	$(2\theta)_2$	$(2\theta)_3$	w_1	w_2
PC								
0%	0.31	0.31	18.0	18.38	20.00	26.70	0.69	0.61
10%	0.30	0.33	18.4	18.35	20.03	26.75	0.69	0.62
30%	0.23	0.33	18.5	18.35	20.00	26.65	0.66	0.58
50%	0.15	0.30	18.8	18.34	20.00	26.68	0.70	0.61
70%	0.07	0.23	19.2	18.44	20.08	26.57	0.82	0.76
TG								
10%	0.30	0.33	18.3	18.33	19.93	26.65	0.70	0.62
30%	0.25	0.35	18.9	18.30	19.92	26.59	0.69	0.60
50%	0.16	0.32	20.0	18.30	19.93	26.66	0.71	0.61
70%	0.06	0.20	20.5	18.39	19.98	26.50	0.60	0.51

The value of the total crystallinity of neat PVdF, w_{cr}, has been estimated to be 0.31.

3.2.1. Copolymer–plasticiser blends

The results from the profile analysis for the blends with 10–70% PC or TG are shown in Table 1. While the total crystallinity (w_{cr}) of the samples diminishes with increasing amount of a plasticiser added to the copolymer matrix, the degree of relative crystallinity, $(w_{cr})_{KF}$, is shown to remain constant in all the samples, except for the two with high concentration of the plasticisers (70 wt%), where the relative crystallinity is a little lower. An analogous trend is shown for the positions of the crystalline reflections ($(2\theta)_1$, and $(2\theta)_2$). For the 70 wt% samples these appear at slightly higher diffraction angles. The constant half-widths of these reflections (w_1 and w_2) suggest the same crystallite sizes in all the samples, except again for those with 70 wt% plasticiser. This indicates that the added plasticisers do not influence the crystalline domains of the copolymer, except at high concentrations.

In contrast to the invariance of the crystalline reflections, the centre position of the amorphous halo ($2\theta_{am}$), moves continually to higher angles as the amount of the plasticisers is increased. This suggests that the composition of the amorphous regions between the crystallites changes when the plasticiser content of the sample varies. Thus, the amorphous phase, in contrast to the crystalline one, is clearly miscible with the plasticisers. Therefore, the increase of the long period with increasing amount of plasticiser observed with SAXS is a result of plasticiser penetrating into the amorphous phase.

The two plasticiser systems differ only marginally in the positions of the amorphous as well as crystalline diffraction peaks. Somewhat higher values of $2\theta_{am}$ for the samples with TG in comparison with those containing PC are probably due to the different chemical composition of these plasticisers.

3.2.2. Copolymer–plasticiser–salt blends

Introduction of the LiTFSI into the gels results in a dramatic change of the crystalline phase (Table 2). The reflections at $2\theta = 18.4$ and 26.7° belonging to the non-polar phase II nearly disappear (Fig. 4c and d). The remaining peak near $2\theta = 20.0°$ must therefore belong to one of the phases I or III (Table 3). As the latter two phases are both polar, it is quite reasonable that they are preferred by the system in the presence of the salt. Only one strong reflection appears in the measured spectral region, and there is only a marginal difference in the positions of this peak for the two phases. Furthermore, the resulting position of the reflection can be influenced by many factors in such a complex system as this one. It is therefore difficult to state with certainty, based on the WAXS data, which of these two modifications really occurs in the current samples. The formation of phase III is more probable though (monoclinic with $a = 8.66$, $b = 4.93$ and c (chain axis) = 2.58 Å, and $\beta = 97°$) [8].

Table 2
Structure parameters of polymer blends with salt added (w_{cr}, overall degree of crystallinity; $(w_{cr})_{KF}$, crystallinity of the PVdF matrix; $2\theta_{am}$, position of an amorphous halo; $2\theta_1$, positions of crystalline reflections; w_1, corresponding half-widths of these reflections (relative scale))

	w_{cr}	$(w_{cr})_{KF}$	$2\theta_{am}$	$(2\theta)_1$	w_1
(LiTFSI + PC)					
10%	0.16	0.17	18.67	20.04	1.18
30%	0.10	0.14	19.00	20.04	1.19
50%	0.08	0.16	18.93	20.13	1.31
70%	0.05	0.17	18.91	20.00	1.32
(LiTFSI + TG)					
10%	0.15	0.17	18.84	20.07	1.34
30%	0.13	0.19	19.25	20.08	1.28
50%	0.11	0.22	19.29	20.15	1.52
70%	0.06	0.20	19.45	20.16	1.49
(LiBF4 + PC)					
30%	0.13	0.19	19.00	20.14	1.25
50%	0.11	0.22	19.40	20.18	1.27
70%	0.07	0.23	19.50	20.16	1.63

Firstly, the experimental value of the position of reflections (200) + (110) is closer to the theoretical one than in the case of the orthorhombic cell of the phase I (see Table 3). Secondly, phase I has been described to occur only when the material has been strained severely [6], which is not the case here as all the films have only been left to dry at room temperature. Finally, the formation of phase III is confirmed by the FTIR data, as discussed below.

Similar observations result when the salt $LiBF_4$ is added instead of LiTFSI (see Table 2 and Fig. 4e). A disappearance of the non-polar phase II is observed as well as a broadening of the crystalline reflections. This suggests that the phase change observed is not entirely due to the well-known plasticizing properties of the TFSI-anion, but may be induced by the polar environment created by other ions as well.

The relative crystallinity, $(w_{cr})_{KF}$, decreases approximately by one third (to around 0.18) as compared to the neat copolymer for all salt containing samples (see Table 2). While the addition of the pure plasticisers to the copolymer does not influence the size of the crystallites in the semicrystalline PVdF, the presence of the salt manifests itself by broadening of the crystalline reflections (w_1 is doubled). This suggests either the formation of smaller crystallites or a less ordered structure of the salt containing system. The centre of the amorphous halo appears at higher angles showing an expected altered composition of the amorphous phase, just as for addition of pure plasticisers.

For the samples with low salt and plasticiser concentration (10 wt%), the presence of phase II (up to a maximum of 15%) can be deduced from the diffractograms (Fig. 4c–e). Thus, this phase seems to disappear only gradually from the crystallites on increasing the addition of the mixture of plasticiser and salt. To confirm the presence of residual phase II in the different samples or to prove conclusively the presence of other phases than II in the samples without salt is not possible with WAXS, since all the reflections overlap in the measured region (see Table 3).

3.3. FTIR

Infrared spectroscopy measurements result in spectra showing bands originating from vibrations of individual bonds or groups in a molecule. This method is thus focusing on the molecular level to a much greater extent than the methods described above. Vibrations such as CH_2 and CF_2 scissoring, rocking and wagging are highly conformation sensitive and therefore the presence or absence of such modes makes it possible to distinguish easily between the different phases occurring in the samples.

Individual bands originating from the different phases were identified according to the literature [28–30]. The presence of phase I in the samples can be ruled out as two strong peaks at 520 and 1280 cm^{-1} representing phase I are absent in all the spectra obtained. On the other hand, peaks at for example 840 and 880 cm^{-1} occurring for phase III are clearly found. In Fig. 5, the spectral region chosen (700–1000 cm^{-1}) imply the presence of both phases II and III in the neat copolymer. A gradual disappearance of phase II with the addition of PC (Fig. 5a), and its total elimination when the salt is added to the system (Fig. 5b), can be followed, as the peaks at 760, 800, 860, and 990 cm^{-1} diminish. On the other hand, the addition of TG seems to suppress the crystallisation of the polar phase III (Fig. 5c), while phase II is conserved. Even in the TG system though, the addition of the salt triggers the crystallisation of the phase III (Fig. 5d). It can thus be concluded, that two different phases (II and III) coexist in the neat copolymer. On addition of a polar medium such as PC, and to an even greater degree the salt, the non-polar phase II is suppressed. The much less polar plasticiser TG does not result in this suppression and allows the non-polar phase II to be retained.

The minor discrepancies observed, the absence of phase II in FTIR samples with 50–70% PC (Fig. 5a), as compared to the results from WAXS, can probably be explained by the variation in the sample thickness used. The FTIR samples must be made very thin (~1 μm) in order to result in a reasonable spectrum. The evaporation of the acetone is comparatively fast and a preferential formation of phase III might occur. It has in fact been reported [29] that the evaporation rate of acetone, when solvent casting the PVdF homopolymer, is a determining factor for the type of crystal form obtained. In the present case, all samples prepared for FTIR have been made under the same conditions and should therefore to a large degree reflect the influence of the solvent type rather than the differences in the acetone evaporation rate.

3.4. DSC

The overall thermal properties of the samples can be investigated by the DSC technique. The glass transition

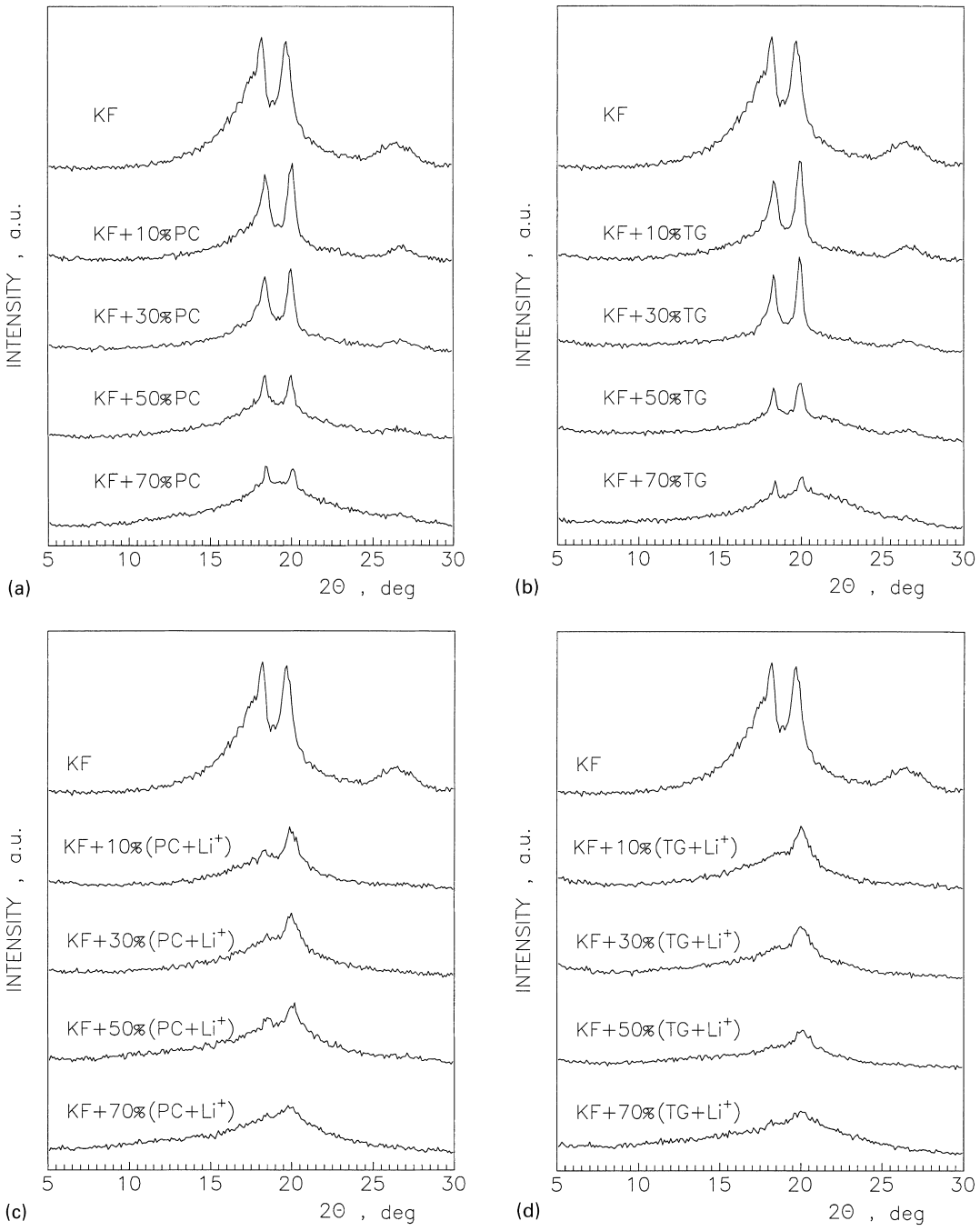

Fig. 4. The diffractograms resulting from the WAXS measurements for the systems with (a) PC; (b) TG; (c) 1 M LiTFSI in PC; (d) 1 M LiTFSI in TG; and (e) 1 M $LiBF_4$ in PC.

temperature, melting point and the thermal stability of the material are all important parameters resulting from the microstructure and morphology of the system. These parameters will for example affect the overall separator properties of the gel electrolyte material when operating in a battery. The mechanical properties will change with temperature, and in unfortunate cases a softening or melting of the electrolyte within the operational temperature regime of the battery could occur and cause a short circuit. The DSC method will also reveal a possible phase separation, which could result in the supposedly conductive medium acting as an insulator. A good indication of the mechanical properties expected of the material can thus be obtained.

The glass transition temperature (T_g) is one of the most important parameters of the amorphous phase for the flexibility of the material at room temperature. The transition spans a very wide temperature range for the neat copolymer, between −130 and −50°C (Fig. 6a), which implies a random distribution of the HFP domains [31]. On plasticiser addition, the transition sharpens and the transition

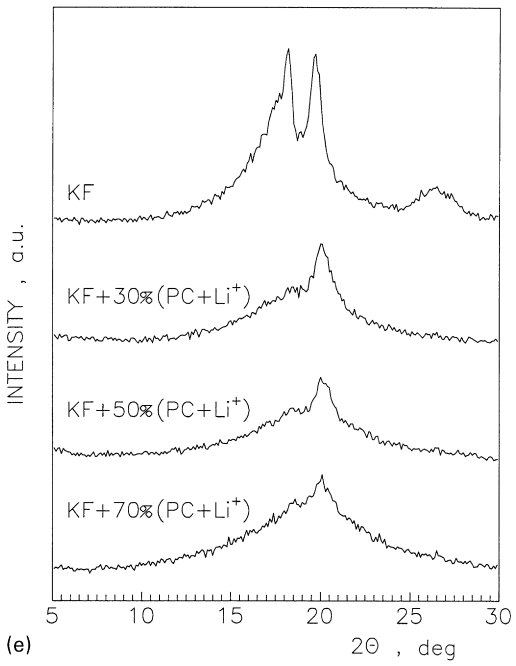

Fig. 4. (*continued*)

temperature is decreasing with increasing plasticiser concentration (Fig. 6b and c and Table 4). The samples thus become both more flexible and better organised, as was also indicated by the slightly narrower reflections shown in Fig. 4a. On salt addition T_g occurs at slightly higher temperatures (Fig. 6d and e). This is due to a larger amount of the amorphous phase being present, but it also suggests some restrictions in the flexibility imposed on the polymer chains.

A clear decrease in melting temperature of the crystalline phase also occurs on plasticiser addition (Table 4). The presence of the salt results in an even more distinct decrease, again demonstrating the great influence the salt imposes on the polymer system.

The presence of crystallisation and melting peaks of pure TG for the sample with 70% of the plasticiser, at −70 and −40°C, respectively, suggest an excess of the component for the composition (Fig. 6d). This result implies a lower miscibility of the polymer with TG than with PC. No such separation of the plasticiser is observed for the PC containing sample.

An endothermic peak occurring at 50°C for PC samples and 55°C for TG samples, isothermal for all compositions, appears most clearly for the mixtures without salt, but only in aged samples (>24 h — shown here). Such a peak has not been detected in freshly prepared samples. This peak together with the melting peak of the crystalline phase is typical of eutectic or peritectic two-phase behaviour [32]. In the present case, we conclude that some kind of peritectic pseudo-equilibrium occurs, since the constant temperature peak appears between the two melting temperatures of the constituents (PVdF − HFP = 130, PC = −100 and TG = −70°C).

Table 3
Positions of crystalline peaks (2θ, °) for different PVDF modifications [8,25] (vs, very strong; s, strong; m, medium strong and w, weak reflection)

I	II	III
–	18.0 vs	–
–	18.4 vs	–
20.8 vs	20.0 vs	20.2 vs
–	26.7 s	–
–	32.3 m	–
36.2 m	36.0 m	35.6 + 36.2 m
–	37.2 m	–
–	38.6 m	–
41.7m	42.0 m	41.7 m
–	46.0 w	–
51.5 w	50.6 w	51.4 w
56.8 w	56.0w	56.8 w

4. Conclusions

Summarising the results presented above, it is clear that adding a polar medium to the PVdF–HFP copolymer may quite strongly affect both structure and, in particular, the morphology of this semicrystalline polymer. This occurs in spite of the fact that this polymer is considered a relatively inert material. Particularly surprising is the fact that introduction into the polymer of a salt solution in PC or TG appears to eliminate the non-polar phase II from the crystallites in favour of the polar phase III. This is in line with observations on PVDF and PVDF gel electrolytes [33–35].

Addition of the pure plasticisers PC and TG primarily affects the amorphous parts of the material, expanding it in a way that can be rationalised using a simple one-dimensional dilution model, involving penetration of the plasticiser into amorphous regions separating crystalline lamellae. From the FTIR data, it is clear that to some extent the crystalline regions are also affected, slightly changing the relative fraction of the two crystalline phases II (non-polar) and III (polar). However, the fraction $(w_{cr})_{KF}$ of the polymer residing in the crystalline regions (about 30 wt%) is not significantly affected by the addition of the pure plasticiser.

Addition of a salt solution in PC or TG to the polymer has a more dramatic effect. First, it eliminates the non-polar phase II from the crystallites in favour of the polar phase III. Secondly, the relative crystallinity $(w_{cr})_{KF}$ is modified substantially, going down to about 20% and at the same time one observes a broadening of the WAXS reflections, indicative of a reduction of crystallite size.

One reason for the behaviour described above could be the different degree of polarity of the polymer chain conformations and the resulting expected difference in the interaction with the ions of the salt. In fact, already in the solution state during the preparation, the presence of ions is expected to favour the more polar conformations

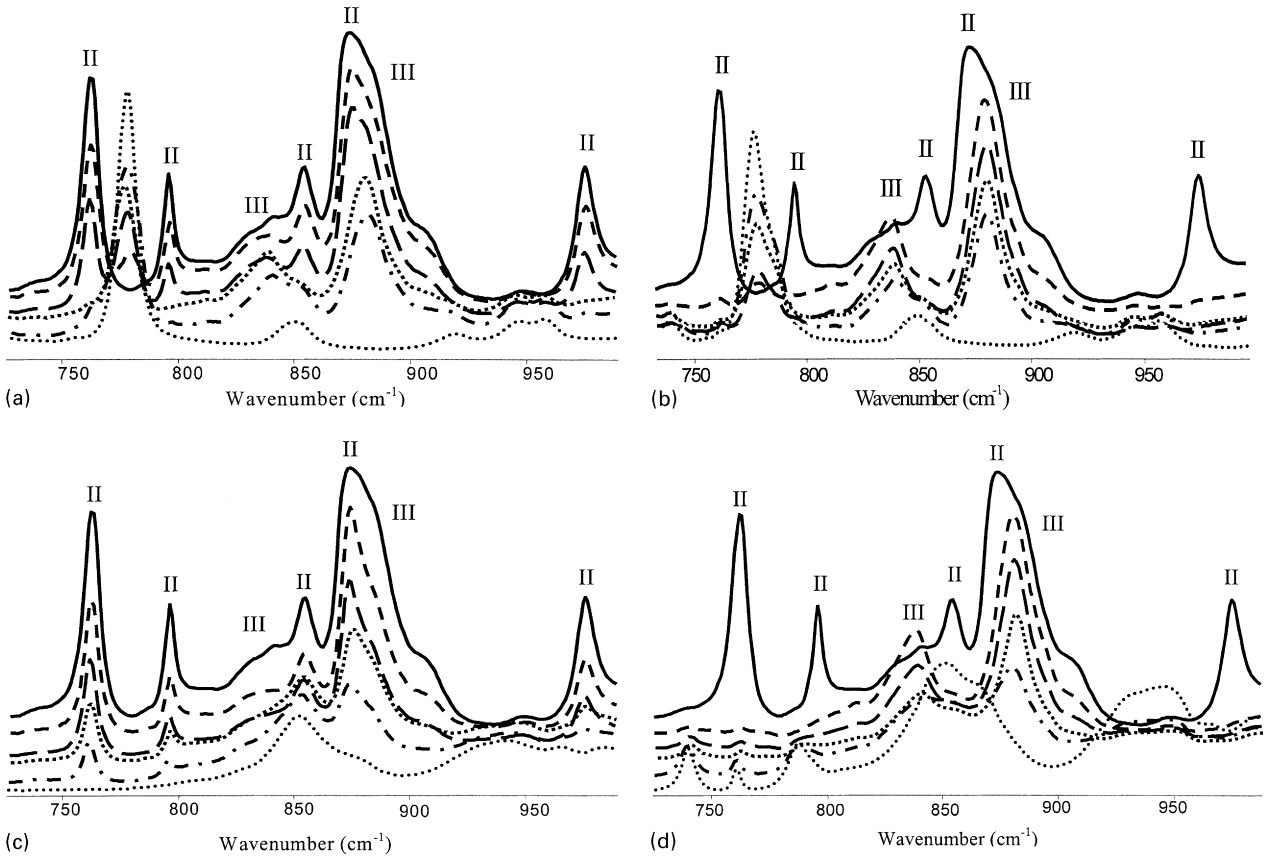

Fig. 5. The FTIR absorption spectra showing the systems with (a) PC; (b) 1 M LiTFSI in PC; (c) TG; (d) 1 M LiTFSI in TG, where the lines represent from above neat copolymer, sample with 10, 30, 50, 70, and 100% plasticiser.

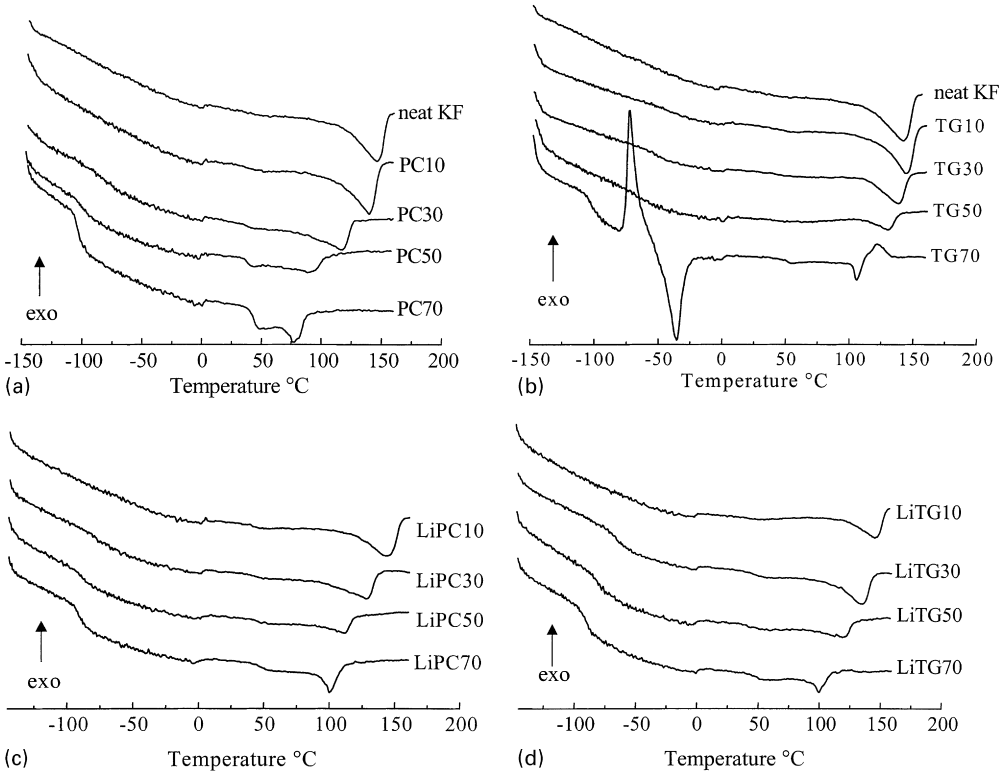

Fig. 6. The DSC graphs showing the system with the copolymer and (a) PC; (b) TG; (c) 1 M LiTFSI in PC; and (d) 1 M LiTFSI in TG.

Table 4
Results from the DSC measurements

Sample	Glass transition interval (°C)	Melting temperature (°C)
Neat copolymer	−160 to −10	125
10% PC	−65 to −45	100
30% PC	−100 to −85	85
50% PC	−105 to −100	80
70% PC	−115 to −105	75
10% TG	−95 to −50	110
30% TG	−100 to −60	105
50% TG	−110 to −90	95
70% TG	−115 to −100	90
10% (1 M LiTFSI + PC)	−65 to −45	110
30% (1 M LiTFSI + PC)	−90 to −55	90
50% (1 M LiTFSI + PC)	−100 to −80	80
70% (1 M LiTFSI + PC)	−105 to −90	75
10% (1 M LiTFSI + TG)	−75 to −45	115
30% (1 M LiTFSI + TG)	−80 to −60	90
50% (1 M LiTFSI + TG)	−90 to −75	85
70% (1 M LiTFSI + TG)	−105 to −90	75

occurring in the crystalline phases I and III. This, in turn, would precondition the polymer chains to form one of these two phases when the solvent evaporates.

It is clear that a combination of the four experimental techniques used here, SAXS, WAXS, FTIR, and DSC, accomplishes a great deal more than any one of them separately, and allows a disentanglement of many of the features in these complex polymer–plasticiser–salt systems.

Acknowledgements

This work has been made possible by the funding from the Royal Swedish Academy of Science, Swedish Natural Science Research Council (NFR), and the Academy of Sciences of the Czech Republic (K 2050602/12).

References

[1] Seiler DA. In: Scheirs J, editor. Modern fluoropolymers, 2nd ed.. Chichester, UK: Wiley, 1998 (chap. 25, p. 487–505).
[2] Tadokoro H. Polymer 1984;25:147–64.
[3] Kawai H. Jpn J Appl Phys 1969;8:975–6.
[4] Hahn BR, Wendorff JH. Polymer 1985;26:1611–8.
[5] Indenherbergh J. Ferroelectrics 1991;115:295–302.
[6] Lando JB, Olf HG, Peterlin A. J Polym Sci 1966;4:941–51.
[7] Doll WW, Lando JB. J Macromol Sci — Phys 1970;4:309–29.
[8] Hasegawa R, Takahashi Y, Chatani Y, Tadokoro H. Polym J 1972;3:600–10.
[9] Cassac GL, Curro JG. J Polym Sci 1974;12:695–702.
[10] Weinhold S, Litt MH, Lando JB. J Polym Sci Polym Lett Ed 1979;17:585–9.
[11] Morra BS, Stein RS. J Polym Sci 1982;20:2261–75.
[12] Tripathy SK, Potenzone JrR, Hopfinger AJ, Banik NC, Taylor PL. Macromolecules 1979;12:656–8.
[13] Gozdz AS, Schmutz CN, Tarascon J-M. US Patent 5,296,318, 1994.
[14] Jiang Z, Carroll B, Abraham KM. Electrochim Acta 1997;42:2667–77.
[15] Gozdz AS, Tarascon JM, Gebizlioglu OS, Schmutz CN, Warren PC, Shokoohi FK. In: Megahed S, Barnett BM, Xie L, editors. Rechargeable Li and Li-ion batteries, Pennington, NJ: The Electrochemical Society, 1995. p. 400 (PV94-28).
[16] Abraham KM, Jiang Z, Carroll B. Chem Mater 1997;9:1978–88.
[17] Choe HS, Giaccai J, Alamgir M, Abraham KM. Electrochim Acta 1995;40:2289–93.
[18] Sen A, Scheinbeim JI, Newman BA. J Appl Phys 1984;56:2433–9.
[19] Tsuchida E, Ohno H, Tsunemi K. Electrochim Acta 1983;28:591.
[20] Tsunemi K, Ohno H, Tsuchida E. Electrochim Acta 1983;28:833.
[21] Abbrent S, Lindgren J, Tegenfeldt J, Furneaux J, Wendsjö Å. J Electrochem Soc 1999;146:3145–9.
[22] Glatter O, Gruber K. J Appl Crystallogr 1993;26:512–8.
[23] Kratky O, Pilz I, Schmitz TJ. J Colloid Interface Sci 1966;21:24–34.
[24] Balta-Calleja FJ, Vonk CG. X-ray scattering of synthetic polymers. Amsterdam: Elsevier, 1989.
[25] Petkov V, Bakalatchev N. J Appl Crystallogr 1990;23:138–40.
[26] Alexander LE. X-ray diffraction methods in polymer science. New York: Wiley-Interscience, 1969.
[27] Lando JB, Doll WW. J Macromol Sci 1968;B2:205–33.
[28] Boerio FJ, Koenig JL. J Polym Sci 1971;Part A-2(9):1517–23.
[29] Tashiro K, Kobayashi M. Phase Trans 1989;18:213–46.
[30] Gregorio R, Cestari M. J Polym Sci 1994;32:859–70.
[31] Sperling LH. Introduction to physical polymer science. 2nd ed.. New York: Wiley, 1992.
[32] McNaughton JL, Mortimer CT. Physical chemistry series 2, vol. 10. London: Butterworths, 1975.
[33] Voice AM, Southall JP, Rogers V, Matthews KH, Davies GR, McIntyre JE, Ward IM. Polymer 1994;35:3363.
[34] Voice AM, Davies GR, Ward IM. Polym Gels Networks 1993;5:123.
[35] Doll WW, Lando JB. J Appl Polym Sci 1970;14:1767.